Transit Signal Priority Enabling Connected and Automated Buses to Cut Through Traffic

Jia Hu, *Member, IEEE*, Zihan Zhang, Yongwei Feng, Zhongxiao Sun, Xin Li, and Xianfeng Yang, *Member, IEEE*

***Abstract*— This research proposes a TSPcut controller that enables connected and automated buses to cut through traffic to make TSP green light. The proposed controller overcomes the shortcomings of conventional TSP strategies and is able to: 1) overtake slowing moving vehicles in order to catch TSP green time; 2) decide the best time to pass the intersection; 3) considering the stochasticity of surrounding traffic; and 4) functional under partially connected and automated environment. It takes full advantage of connected vehicle technology by taking in real-time vehicle and infrastructure information as optimization input. The problem is formulated as an SMPC problem and is solved by a high-efficient dynamic programming algorithm. The nonlinear bicycle model is adopted as the system dynamics to realize CAV bus's lane-changing and overtaking function. The stochasticity of surrounding traffic is considered as a probability distribution which is transformed into a linear chance constraint. Simulation evaluation is conduct to compare the TSPcut against NTSP, CTSP and BocTSP. Sensitive analysis is conducted for congestion levels. The evaluation results demonstrate that the TSPcut improves the bus delay reduction by 17.9%–49.1%, and the benefits are 3.5% to 16.1% greater than that of other TSP systems. The range is caused by different congestion levels. In addition. Further tests are conducted to analyze how CAV bus's arrival time and the speed of background traffic influence the performance of the TSPcut.**

***Index Terms*— Transit signal priority, optimal control, stochastic model predictive control, connected and automated bus.**

I. Introduction

WITH the growth of the population and the increase of private automobiles, the world is facing tremendous pressure caused by the road transportation system, such as traffic congestion, energy consumption and pollution. Reliable public transit service is able to free up space on the roads and reduce demand for fossil fuels [1]. Therefore, the strategies that could improve public transit service are in great need.

Transit Signal Priority (TSP) is one of the most effective countermeasures. It is a signal control strategy that modifies traffic signal timing or phasing according to bus arrivals. By adjusting traffic signal plan, the transit bus delay at signalized intersection is reduced, thus the public transit service achieves improvement and bus ridership increases. The TSP technology has been widely applied in many major cities all over the world, such as Seattle, Los Angeles, Oakland, Chicago and Vancouver. In these cities, transit travel time is reduced by 9% to 50% [1]–[3]. It has been demonstrated that TSP strategy is able to significantly promote public transportation system.

The TSP strategy was developed back in the late 1960s [4]. The early TSP strategies include extending originally planned green time and early ending the current red phase. These two strategies are Conventional TSP (CTSP) called 'green extension' and 'red truncation' [5]. The problem of CTSP is that it not only disturbs the progression on the competing movements and reduces the capacity of the competing travel direction but also covers only a small portion of buses on the TSP direction. According to Chatila and Swenson [6], only up to 20% buses can benefit from CTSP. This drawback mainly due to two reasons. One is that in rush hours, queue discharging on the TSP direction takes up much green time, and has an adverse impact on buses. Another is that the bus cannot adjust its motion status according to current signal timing information and traffic condition. Because of these problems, the CTSP can only cover a limited portion of buses and the TSP green time cannot be fully utilized.

To overcome the shortcomings of the CTSP, various new mechanisms are proposed [7]–[13]. However, these mechanisms still belong to green extension or red truncation. This feature limits the effectiveness of the TSP. Therefore, numbers of research have been committed to developing advanced TSP logics, such as phase insertion [14], cycle extension [15], phase skipping, green reallocation, and adaptive TSP [3], [16]. All these new TSP logics can increase the portion of buses served and reduce the adverse effects on the competing movements. However, new strategies only change the control logic, but neglect the main influencing factors, including traffic condition and the adjustment of bus's own status. Some studies assume exclusive bus lanes [17] and neglect the impacts of queue

Manuscript received 27 March 2020; revised 19 October 2020 and 16 March 2021; accepted 28 May 2021. Date of publication 30 August 2021; date of current version 8 July 2022. This work was supported in part by the National Natural Science Foundation of China under Grant 61803284 and Grant 61903058, in part by the Shanghai Oriental Scholar in 2018, in part by the Shanghai Yangfan Program under Grant 18YF1424200, in part by the Tongji Zhongte Chair Professor Foundataion under Grant 000000375-2018082, and in part b the National Key Research and Development Program of China under Grant 2018YFB1600600 and Grant 2019YFB160402. The Associate Editor for this article was M. Mesbah. *(Corresponding author: Xin Li.)*

Jia Hu, Zihan Zhang, and Yongwei Feng are with the Key Laboratory of Road and Traffic Engineering, Ministry of Education, Tongji University, Shanghai 200092, China (e-mail: hujia@tongji.edu.cn; zihan_zhang9549@163.com; 1651373@tongji.edu.cn).

Zhongxiao Sun is with Tenew Automotive Technology (Suzhou) Company Ltd., Suzhou 401122, China (e-mail: hyo.sun@tnchassis.com).

Xin Li is with the College of Transportation Engineering, Dalian Maritime University, Dalian 116026, China, and also with the Collaborative Innovation Center for Transport Study, Dalian Maritime University, Dalian 116026, China (e-mail: xtopli@dlmu.edu.cn).

Xianfeng Yang is with the Department of Civil & Environmental Engineering, The University of Utah, Salt Lake City, UT 84112 USA (e-mail: x.yang@utah.edu).

Digital Object Identifier 10.1109/TITS.2021.3086110

This work is licensed under a Creative Commons Attribution 4.0 License. For more information, see https://creativecommons.org/licenses/by/4.0/

and obstacle vehicles [18]. Furthermore, in the majority of research, it is assumed that buses maintain constant speed. In fact, exclusive bus lanes are not designed on many urban streets, which conflicts with constant bus speed assumption and limits the effectiveness of TSP systems.

The reason why existing TSP strategies do not consider traffic condition and bus status is that complete and reliable information is unavailable, such as signal timing and surrounding traffic. However, with the emerging of Connected and Automated Vehicle (CAV) technology, accurate measurement, information collection and auto-driving become available. In addition, a SPaT (Signal Phase and Timing) Challenge [19] has been activated by the USDOT (U.S. Department of Transportation) to encourage collaboration between federal, state and local stakeholders on the deployment of DSRC infrastructure with SPaT broadcasts. The challenge received great attention. Within a year, a total of 26 states have committed with 216 operating signals on over thirty corridors. Based on these advanced technologies, two-way communication between bus and signal controller, bus status measurement, and traffic condition detection can be realized. Hu has taken full advantage of the new technologies and proposes next generation TSP logic based on Connected Vehicles Technology (TSPCV) [20], but this TSP strategy cannot optimize state trajectory of buses. Therefore, considering the emerging technologies and the shortcoming of the existing research, developing a new TSP controller is a necessity.

Existing TSP controllers seldomly take traffic condition into consideration, including the stochasticity of the surrounding traffic. It is against the fact that unlike CAVs, the maneuvers of Human-driven Vehicles (HV) are not determined, and the mixed traffic flow of CAVs and HVs will last for at least a decade [21]. Therefore, lack of consideration of the stochasticity may lead to potential collisions. Nowadays, most automotive control research adopts Model Predictive Control (MPC) [22]–[25]. The advantage of MPC is that it can integrate predicting forward information to generate a series of optimal control commands best achieving certain objectives while satisfying constraints on inputs and states. However, the conventional MPC is unable to consider stochastic factors. Stochastic Model Predictive Control (SMPC) [26], [27] has been proposed to address this defect. Probability distribution is introduced to describe stochasticity. Therefore, to consider the effect of traffic on buses and to avoid collisions, there is potential to apply the theories of SMPC to guide buses through intersections with TSP.

Furthermore, to deal with the impedance from the surrounding traffic, the TSP controller does not only need to consider the stochasticity, but also needs to have the overtaking capability. Most CAV controllers are automated only in the longitudinal direction [28]–[31]. However, the surrounding traffic would have a great adverse effect on the controller with only longitudinal automation. For instance, if a low-speed HV is traveling right in front of the ego CAV bus, given the controller function is only longitudinal automation, the ego CAV bus would have to slow down following the HV. On the contrary, if the ego CAV bus is able to make a lane change and overtake the low-speed HV, the bus will have chance to make through the signal light and improve the fuel saving. Therefore, it is necessary to automate both longitudinally and laterally.

For most MPC controllers, the optimization time horizon is fixed [24], [32], [33]. It means that the conventional controllers cannot take signal timing plan into consideration. In order to coordinate with the TSP timing plan, the optimization time horizon of CAV-bus controller shall be able to be adjusted in real time according to the TSP green time and queuing status. The variable time horizon design enables a CAV-bus to catch TSP green light, and reduce delay at a signalized intersection. Hence, it is critical for a CAV-bus controller to have a dynamic optimization time horizon.

Given the shortcomings of the existing TSP logics, and the emerging technologies, this research proposes a TSP controller that enables CAV buses to cut through traffic (TSPcut). This controller is applicable to a single CAV bus approaching an isolated signalized intersection. It is able to take full advantage of TSP green time and bears the following features:

- Able to overtake slow moving vehicles in order to catch TSP green time;
- Able to decide the best time to pass the intersection;
- Considering the stochasticity of surrounding traffic;
- Functional under partially connected and automated environment.

The remainder of this paper is organized as follows. Section II describes the research scope and highlights. Section III provides detailed formulation of the proposed controller. Section IV identifies all the specifics of the evaluation and presents its results and findings. Section V concludes this research and discusses future research.

II. Research Scope

The goal of the TSPcut is to take full advantage of the TSP green time and to reduce the bus delay and fuel consumption at signalized intersections. There are three highlights of the proposed controller:

Catching green light without waiting for 'Grandma Drivers': the TSPcut is able to guide buses to overtake those "grandma drivers" when they obstruct the CAV bus. Lane-changing and overtaking maneuvers enable the CAV bus to bypass the slow-moving traffic flow ahead, thus is able to reduce the waste of TSP green time. The smoother and more continuous motion can save extra fuel for the bus and make the passengers on board feel more comfortable.

Improving safety by considering the stochasticity of background traffic: in mixed traffic, the stochasticity of HVs can increase the risk of collision, thus the proposed controller introduces probability distributions to describe stochasticity and formulate it into linear constraints. Safety is significantly improved for CAV buses passing through mixed traffic flow.

Reducing bus delay by deciding the best time to pass the intersection: the TSPcut adopts dynamic optimization time horizon. It means that the duration of travelling is optimized in real time by considering current TSP green time and queuing. The TSP timing plan can be fully utilized and the unnecessary bus delay is reduced.

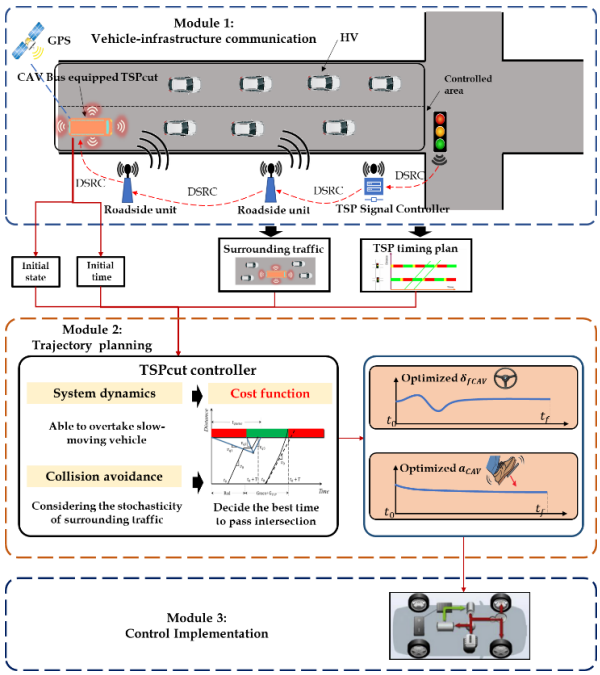

Fig. 1. TSPcut logic.

The TSPcut logic is presented in Fig.1. This logic aims to achieving a cooperation between CAV bus and TSP green time via V2I communication. The proposed TSPcut controller could optimize the CAV bus's trajectory and control its motion based on the real-time information of background traffic and signal timing plan. The goal is to take full use of TSP green time and increase the portion of buses served.

The TSPcut logic is divided into three modules. Module 1 addresses the communication between vehicles and infrastructures. Module 2 and module 3 achieve the functions of the proposed controller. The research scope of this paper focuses on module 2.

Module 1: As shown in Fig. 1, the controlled area is defined as the communication range of the roadside units. In this area, the traffic condition and the signal timing plan are transmitted through vehicle-infrastructure communication. The system requires the following equipment: i) GPS installed on the CAV buses; ii) communication devices installed on CAV buses, traffic lights and other road units to enable communication between vehicles and infrastructures.

Module 2: When the central controller detects that the ego bus's GPS location has just entered the controlled area, the TSP system is activated and determines whether it is eligible for the ego bus to be granted with TSP. The initial state of the bus, state of the preceding vehicles, and TSP timing plan collected in module 1 are used as input and fed into the controller. The controller then starts to optimize eco CAV bus's travel trajectory and to adjust its travel duration in order to reduce bus delays and improve fuel savings. The trajectory is then transmitted to the CAV bus as the control commands and are also stored for future use.

Module 3: The CAV bus receives command from the proposed controller and adjusts its states accordingly.

TABLE I
INDICES AND PARAMETERS

a_x	Ego CAV bus's commanded longitudinal acceleration (m/s^2)
y	Lateral position error between ego CAV bus and lane centerline (m)
l_*	Distance between vehicle's gravity center and front or rear axles (m)
n	Number of obstacle vehicles running in the range of ego CAV bus's detection
t_0	The initial time when the controller is activated (s)
T	The travel duration approaching the intersection (s)
τ	Time step (s)
x	Ego CAV bus's longitudinal position along the road (m)
$sd^{(i)}$	Distance between ego CAV bus and ith obstacle vehicle (m)
$\boldsymbol{u}$	System dynamics' control vector
v	Ego CAV bus's longitudinal speed (m/s)
$\dot{x}^{(i)}$	Longitudinal speed of ith obstacle vehicle (m/s)
$\Delta x^{(i)}$	The longitudinal distance between the ith obstacle vehicle and ego bus (m)
$\Delta \boldsymbol{x}$	Set of $\Delta x^{(i)}$
$\dot{y}$	Ego CAV bus's lateral speed (m/s)
$\dot{y}^{(i)}$	Lateral speed of ith obstacle vehicle (m/s)
$\Delta y^{(i)}$	The lateral distance between the ith obstacle vehicle and ego CAV bus (m)
$\Delta \boldsymbol{y}$	Set of $\Delta y^{(i)}$
δ_f	Ego CAV bus's commanded front steering angle (rad)
$\mu_l^{(i)}$	Mean of ith obstacle vehicle's longitudinal speed distribution
$\mu_w^{(i)}$	Mean of ith obstacle vehicle's lateral speed distribution
$\boldsymbol{z}$	System dynamics' state vector
$\boldsymbol{z}_d$	Deterministic component of system dynamics' state vector
$\boldsymbol{z}_s$	Stochastic component of system dynamics' state vector
$\sigma_l^{2(i)}$	The variance of ith obstacle vehicle's longitudinal speed distribution
$\sigma_w^{2(i)}$	The variance of ith obstacle vehicle's lateral speed distribution
ψ	Ego CAV bus's yaw angle (rad)
C	The signal cycle length (s)
R	The red time (s)
G	The green time (s)
G_{TSP}	The TSP green time (s)
$\boldsymbol{\omega}$	Stochasticity concerned vector
v_{q1}	Speed of queuing shockwave (m/s)
v_{q2}	Speed of discharging shockwave (m/s)
v_{q3}	Speed of departure shockwave (m/s)
L	The distance from to the initial position of ego bus to the stop bar (m)
Q_0	The initial queue length when the red light just turns on (m)

III. PROBLEM FORMULATION

The formulation of the TSPcut is presented. The controller is formulated as an optimal control. The kinematic bicycle model is adopted as the system dynamics in order to achieve automatic lane-changing and overtaking. It enables the ego CAV bus to overtake slowing moving vehicles to catch TSP green time.

The cost function is designed to reduce bus delays and to improve fuel savings. The optimization horizon is adjusted in real time according to the current signal timing and background traffic. It could help the ego CAV bus decide the best time to pass an intersection.

A chance constraint considering the stochasticity of surrounding traffic is introduced to ensure collision-free.

Table I lists the indices and parameters utilized hereafter:

A. State Definition

Definition 1: Longitudinal distance $\Delta x^{(i)}$ is defined as the difference between the ith obstacle vehicle's longitudinal position $x^{(i)}$ and the ego bus's longitudinal position x. $\boldsymbol{\Delta x}$ is the set of $\Delta x^{(i)}$:

$$\Delta x^{(i)} = x^{(i)} - x \tag{1}$$

$$\boldsymbol{\Delta x} = [\Delta x^{(1)}, \Delta x^{(2)}, \ldots \Delta x^{(i)} .., \Delta x^{(n)}] \tag{2}$$

Definition 2: Lateral distance $\Delta y^{(i)}$ is defined as the difference between the ith obstacle vehicle's lateral position $y^{(i)}$ and the ego bus's lateral position y. $\boldsymbol{\Delta y}$ is the set of $\Delta y^{(i)}$:

$$\Delta y^{(i)} = y^{(i)} - y \tag{3}$$

$$\boldsymbol{\Delta y} = [\Delta y^{(1)}, \Delta y^{(2)}, \ldots \Delta y^{(i)} .., \Delta y^{(n)}] \tag{4}$$

Definition 3: The system state vector $\boldsymbol{z}$ and control vector $\boldsymbol{u}$ are defined as follows:

$$\boldsymbol{z} = [x, y, \psi, \upsilon, \boldsymbol{\Delta x}, \boldsymbol{\Delta y}]^T \tag{5}$$

$$\boldsymbol{u} = [\delta_f, a_x]^T \tag{6}$$

B. System Dynamics

For achieving automatic lane-changing and overtaking function, this research adopts kinematic bicycle model [34] as the system dynamics of the bus and obstacle vehicles. Some assumptions are proposed to linearize this bicycle model to reduce computation burden.

The system states of the ego bus, such as x, y, ψ, υ are explained in Fig.2. β is the angle of the current velocity of gravity center with respect to the longitudinal axis of the vehicle. l_f, l_r denotes the distance between vehicle's gravity center and front or rear axles.

Definition 4: The nonlinear bicycle model is formulated as follows:

$$\begin{aligned} \dot{x} &= \upsilon cos(\psi + \beta) \\ \dot{y} &= \upsilon sin(\psi + \beta) \\ \dot{\psi} &= \frac{\upsilon}{l_r} sin\beta \\ \dot{\upsilon} &= a_x \\ \beta &= tan^{-1}(\frac{l_r}{l_f + l_r} tan\delta_f) \end{aligned} \tag{7}$$

Assumption 1: δ_f, ψ and β are small, thus the following assumption is adopted:

$$\beta \approx \frac{l_r}{l_f + l_r}\delta_f, \quad sin\beta \approx \beta, \ cos(\psi + \beta) \approx 1, \\ sin(\psi + \beta) \approx \psi \tag{8}$$

Theorem 1: The linear system dynamics are formulated as follows:

$$\begin{aligned} \dot{\boldsymbol{z}} &= \boldsymbol{A}\boldsymbol{z} + \boldsymbol{B}\boldsymbol{u} + \boldsymbol{D}\boldsymbol{\omega} \\ \boldsymbol{\omega} &= [\dot{x}^{(1)}, \ldots, \dot{x}^{(n)}, \dot{y}^{(1)}, ..., \dot{y}^{(n)}]^{\boldsymbol{T}} \\ \boldsymbol{A} &= \begin{bmatrix} 0 & 0 & 0 & 1 & \boldsymbol{0}_{1\times 2n} \\ 0 & 0 & \upsilon & 0 & \boldsymbol{0}_{1\times 2n} \\ 0 & 0 & 0 & 0 & \boldsymbol{0}_{1\times 2n} \\ 0 & 0 & 0 & 0 & \boldsymbol{0}_{1\times 2n} \\ 0 & 0 & 0 & -\boldsymbol{I}_{n\times 1} & \boldsymbol{0}_{n\times 2n} \\ 0 & 0 & -\upsilon \boldsymbol{I}_{n\times 1} & 0 & \boldsymbol{0}_{n\times 2n} \end{bmatrix} \\ \boldsymbol{B} &= \begin{bmatrix} 0 & 0 \\ 0 & 0 \\ \frac{\upsilon}{l_f + l_r} & 0 \\ 0 & 1 \\ \boldsymbol{0}_{2n\times 1} & \boldsymbol{0}_{2n\times 1} \end{bmatrix} \\ \boldsymbol{D} &= \begin{bmatrix} \boldsymbol{0_{4\times 2n}} \\ \boldsymbol{E_{2n\times 2n}} \end{bmatrix} \end{aligned} \tag{9}$$

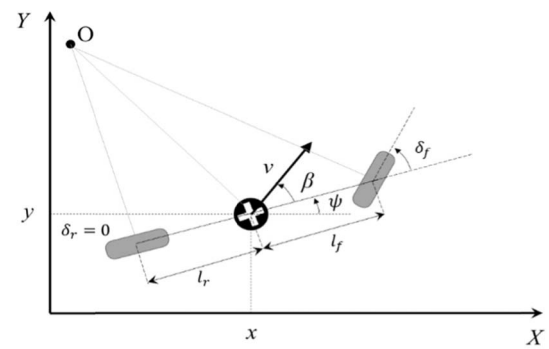

Fig. 2. Nonlinear bicycle model notation.

where $\boldsymbol{I}$ is a vector, all the components of which are one. $\boldsymbol{0}$ is a zero matrix. $\boldsymbol{E}$ is a unit matrix. $\boldsymbol{z}$ and $\boldsymbol{u}$ are defined as **Definition 3**. $\boldsymbol{\omega}$ is a stochasticity concerned vector which is introduced to describe random variable $\dot{x}^{(i)}$ and $\dot{y}^{(i)}$.

Proof: According to ***Assumption 1***, the linearized bicycle model is formulated as follows:

$$\begin{aligned} \dot{\boldsymbol{\xi}} &= \boldsymbol{A_1}\boldsymbol{\xi} + \boldsymbol{B_1}\boldsymbol{u} \\ \boldsymbol{\xi} &= [x, y, \psi, \upsilon]^{\boldsymbol{T}} \\ \boldsymbol{A_1} &= \begin{bmatrix} 0 & 0 & 0 & 1 \\ 0 & 0 & \upsilon & 0 \\ 0 & 0 & 0 & 0 \\ 0 & 0 & 0 & 0 \end{bmatrix} \\ \boldsymbol{B_1} &= \begin{bmatrix} 0 & 0 \\ 0 & 0 \\ \frac{\upsilon}{l_f + l_r} & 0 \\ 0 & 1 \end{bmatrix} \end{aligned} \tag{10}$$

In addition, the state variable $\boldsymbol{\Delta x}$ and $\boldsymbol{\Delta y}$ including the information of obstacle vehicles should be considered into the system dynamics, and according to **Definition 1**, $\boldsymbol{\Delta \dot{x}}$ is inferred as follows:

$$\boldsymbol{\Delta \dot{x}} = [\Delta \dot{x}^{(1)}, \Delta \dot{x}^{(2)}, \ldots, \Delta \dot{x}^{(i)}, \ldots, \Delta \dot{x}^{(n)}]^{\boldsymbol{T}} \tag{11}$$

$$\Delta \dot{x}^{(i)} = \dot{x}^{(i)} - \upsilon \tag{12}$$

According to **Definition 2**, $\boldsymbol{\Delta \dot{y}}$ is inferred as follows:

$$\boldsymbol{\Delta \dot{y}} = [\Delta \dot{y}^{(1)}, \Delta \dot{y}^{(2)}, \ldots, \Delta \dot{y}^{(i)}, \ldots, \Delta \dot{y}^{(n)}]^T \tag{13}$$

$$\Delta \dot{y}^{(i)} = \dot{y}^{(i)} - \dot{y} = \dot{y}^{(i)} - \upsilon\psi \tag{14}$$

Based on (10)-(14), **Theorem 1** can be proved. ■

C. Cost Function

The objective of the optimization is to reduce bus delay and to save fuel consumption. The cost function is defined as follows:

$$J = \int_{t_0}^{t_0+T} (\frac{\beta_0}{2} u^T u + \frac{\beta_1}{2}\psi^2 + \frac{\beta_2}{2}(\upsilon - \upsilon_0)^2) dt \\ + \frac{\beta_3}{2}(x(T) - L)^2 + \frac{\beta_4}{2}(\upsilon(T) - \upsilon_0)^2 \tag{15}$$

$$\beta_0, \beta_1, \beta_2, \beta_3, \beta_4 > 0, \quad if \ (t_0, \upsilon_0) \in \Omega \tag{16}$$

$$\beta_0, \beta_1, \beta_3 > 0, \quad \beta_2 = 0, \ \beta_4 = 0, \ if \ (t_0, \upsilon_0) \notin \Omega \tag{17}$$

$$\Omega = \left\{ (t_0, \upsilon_0) | t_{queue} \leq t_0 + \frac{L}{\upsilon_0} \leq C + G_{TSP} \right\} \tag{18}$$

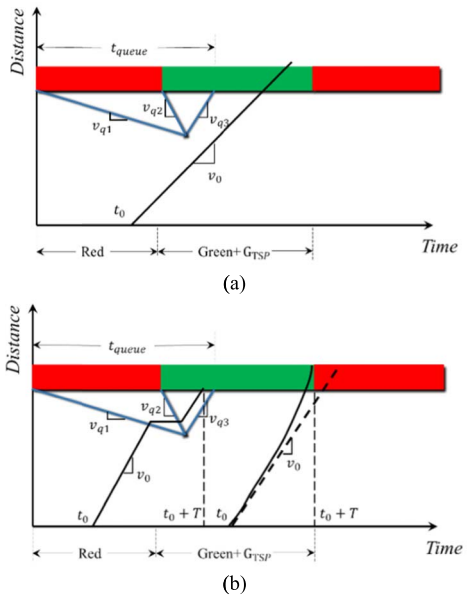

Fig. 3. The bus's state trajectories approaching the signalized intersection.

where β_0, β_1, β_2 are weighting factors in the running cost; β_0, β_1 guarantee the fuel saving and smooth trajectory. β_3 and β_4 ensure a constraint on vehicle's final state. However, the values of the weighting factors will be changed with respect to the values of t_0 and v_0. As shown in Fig.3(a), when $(t_0, v_0) \in \Omega$, the ego bus is able to catch the green light at a constant speed. In this state, bus delay is zero and fuel consumption is minimized. For maintaining this motion state, β_2 and β_4 must be positive values. As depicted in Fig.3(b), when $(t_0, v_0) \notin \Omega$, due to queuing or inadequate TSP green time, the ego bus cannot pass through the stop bar at a constant speed and must adjust its motion state to reduce delay. Therefore, in these two scenarios, β_2 and β_4 are equal to zero, and optimization time horizon depends on rest green time or queuing time. The formulation of queuing time is described in the following. Detailed derivation is provided in [35], [36]:

$$t_{queue} = \frac{Q_0 + Rv_{q2}}{v_{q2} - v_{q1}} + \frac{Q_0 v_{q2} + Rv_{q1}v_{q2}}{(v_{q2} - v_{q1})v_{q3}} \tag{19}$$

D. Constraints and Initial Conditions

The problem is constrained by system dynamics, speed limit, geometry boundaries, control variables range and collision avoidance. The system dynamics constraints are presented in the section 'System dynamics'. The stochasticity of surrounding traffic is accommodated in the collision avoidance constraint.

1) Speed Limit: Longitudinal speed should never exceed the speed limit. This constraint can be specified as:

$$v_{min} \leq v \leq v_{max} \tag{20}$$

2) Geometry Boundaries: The bus should be driven within road geometry boundaries:

$$y_{min} \leq y \leq y_{max} \tag{21}$$

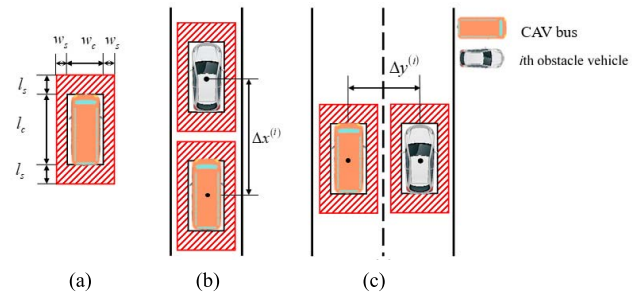

Fig. 4. Vehicle safe area definition.

3) Control Variables Range: The ego bus's acceleration should be reasonable considering vehicle performance and comfort, and steering angle should be within its steering range:

$$\begin{aligned} a_{xmin} &\leq a_x \leq a_{xmax} \\ \delta_{fmin} &\leq \delta_f \leq \delta_{fmax} \end{aligned} \tag{22}$$

4) Collision Avoidance: Constraints that ensure collision-free are detailed in Theorem 1. The definition of collision-free is for the ego CAV bus to keep a certain user-defined safety distance from other vehicles. This subsection presents one key feature of this research which introduces stochasticity consideration of the surrounding traffic into problem formulation as a probability. This subsection also demonstrates how the introduced probability distribution can be simplified into linear form to enable real-time application.

Assumption 2: the stochasticity comes from the obstacle vehicles' longitudinal speed $[\dot{x}^{(1)}, \ldots \dot{x}^{(i)}, \ldots \dot{x}^{(n)}]^T$ and lateral speed $[\dot{y}^{(1)}, \ldots \dot{y}^{(i)}, \ldots \dot{y}^{(n)}]^T$. It is assumed that the longitudinal and lateral speed of ith obstacle vehicle both obey the Gaussian distribution:

$$\dot{x}^{(i)} \sim N(\mu_l^{(i)}, \sigma_l^{2(i)}) \tag{23}$$

$$\dot{y}^{(i)} \sim N(\mu_w^{(i)}, \sigma_w^{2(i)}) \tag{24}$$

where subscript l denotes longitudinal notation and subscript w denotes lateral notation.

Definition 5: As shown in Fig.4, vehicle's safe area is defined as a rectangle. The safe distance between the ego CAV and ith obstacle vehicle is defined as follows:

$$\begin{aligned} \Delta x_{safe} &= \frac{l_c^{(i)} + l_c}{2} + max\{l_s, l_s^{(i)}\} \text{ or} \\ \Delta y_{safe} &= \frac{w_c^{(i)} + w_c}{2} + max\{w_s, w_s^{(i)}\} \end{aligned} \tag{25}$$

l_s and w_s are the longitudinal and lateral safe distance of the ego CAV. $l_s^{(i)}$ and $w_s^{(i)}$ are ith obstacle vehicle's longitudinal and lateral safe distance. Ego CAV's length and width are denoted as l_c and w_c.

Proposition 1: given $p \in [0.5, 1)$, at every time step, following chance constraint must be satisfied to ensure user-defined safety standard:

$$Pr((\boldsymbol{g}^{(i)})^T \boldsymbol{z_{k+1}} \leq h^{(i)}) \geq p \tag{26}$$

where,

$$\begin{cases} \boldsymbol{g}_l^{(i)} = [\underbrace{0, 0, \ldots, 0}_{i+5}, -1, \underbrace{0, \ldots, 0}_{2n-i}]^T, \quad h_l^{(i)} = -\Delta x_{safe} \\ \boldsymbol{g}_w^{(i)} = [\underbrace{0, 0, \ldots, 0}_{n+5+i}, -1, \underbrace{0, \ldots, 0}_{n-i}]^T, \quad h_w^{(i)} = -\Delta y_{safe} \end{cases} \tag{27}$$

p is a risk management parameter. It represents the balance between safety and efficiency. A large value of p leads to conservative driving behavior. On the other hand, a low value of p leads to more aggressive driving behavior, which increases the risk of collision. There is no perfect answer to the value of p. Future users could pick their own p according to preferences.

Proof: the following proof takes longitudinal control as an example. The proof on the lateral dimension is very similar and hence omitted from this paper:

$$(\boldsymbol{g}_l^{(i)})^T z_{k+1} = -\Delta x_{k+1}^{(i)} = s_{k+1} - s_{k+1}^{(i)} \tag{28}$$

The collision avoidance requires that vehicles will not collide at next time step k+1. Hence, the longitudinal distance must be larger than the safety distance and the following equality must be satisfied:

$$\Delta x_{k+1}^{(i)} = s_{k+1}^{(i)} - s_{k+1} \geq \Delta x_{safe} \tag{29}$$

According to equation (28) and inequality (29), the following constraint can be derived:

$$(\boldsymbol{g}_l^{(i)})^T z_{k+1} \leq h_l^{(i)} \tag{30}$$

Based on ***Assumption 2***, given the stochasticity in state vector z, a tunable risk probability p is introduced into inequality (30). Therefore, the constraint is transformed into a chance constraint and **Proposition 1** has been proved. ■

For linearizing the safety chance constraint, **theorem 2** is proposed to address this problem.

Theorem 2: The linear collision avoidance constraint in this paper is formulated as follows:

$$(\boldsymbol{g}_l^{(i)})^T z_{d,k+1} \leq h_l^{(i)} - \gamma_l^{(i)} \text{ or } (\boldsymbol{g}_w^{(i)})^T z_{d,k+1} \leq h_w^{(i)} - \gamma_w^{(i)} \tag{31}$$

where,

$$z_{d,k+1} = [\dot{x}_{k+1} \quad \dot{y}_{k+1} \quad \dot{\varphi}_{k+1} \quad e_{\varphi,k+1} \quad e_{y,k+1} \quad s_{k+1} \quad -s_{k+1}\boldsymbol{I}_{1\times n} \quad -e_{y,k+1}\boldsymbol{I}_{1\times n}]^T \tag{32}$$

$$z_{s,k+1} = [0 \quad 0 \quad 0 \quad 0 \quad 0 \quad 0 \quad s_{k+1}^{(1)} \ldots s_{k+1}^{(n)} \quad e_{y,k+1}^{(1)} \ldots e_{y,k+1}^{(n)}]^T \tag{33}$$

$$\gamma_{k,l}^{(i)} = F_{k,l}^{(i)-1}(p) \tag{34}$$

$$\gamma_{k,w}^{(i)} = F_{k,w}^{(i)-1}(p) \tag{35}$$

$F_{k,l}^{(i)}(\bullet)$ is the distribution function of $-s_{k+1}^{(i)}$, $F_{k,w}^{(i)}(\bullet)$ is the distribution function of $-e_{y,k+1}^{(i)}$, and $F_{k,*}^{(i)-1}(\bullet)$ is the inverse function of $F_{k,*}^{(i)}(\bullet)$, $* \in \{l, w\}$."

Proof: Following formulations prove **Theorem 2**. The proof takes longitudinal control as an example.

To linearize the chance constraint (26), system state vector at time $k+1$ $\mathbf{z}_{k+1}$ can be divided into a deterministic component $\mathbf{z}_{\mathrm{d,k+1}}$ and a stochastic component $\mathbf{z}_{\mathrm{s,k+1}}$:

$$z_{k+1} = z_{s,k+1} + z_{d,k+1} \tag{36}$$

According to inequality (30) and equation (36), the following equations can be inferred:

$$\left(\boldsymbol{g}_l^{(i)}\right)^T \left(z_{s,k+1} + z_{d,k+1}\right) = s_{k+1} - s_{k+1}^{(i)} \leq h_l^{(i)} \tag{37}$$

$$\left(\boldsymbol{g}_l^{(i)}\right)^T z_{d,k+1} = s_{k+1} \tag{38}$$

$$\left(\boldsymbol{g}_l^{(i)}\right)^T z_{s,k+1} = -s_{k+1}^{(i)} \tag{39}$$

Based on **Proposition 2**, the stochasticity of the chance constraint comes from the stochastic component $z_{\mathrm{s,k+1}}$, thus $\left(\boldsymbol{g}_l^{(i)}\right)^T z_{s,k+1}$ is in compliance with a probability distribution:

$$Pr((\boldsymbol{g}_l^{(i)})^T z_{s,k+1} \leq \gamma_{k,l}^{(i)}) = F_{k,l}^{(i)}(\gamma_{k,l}^{(i)}) = p \tag{40}$$

Given inequality (37) and equation (40), the following inequality can be derived:

$$(\boldsymbol{g}_l^{(i)})^T z_{k+1} - \left(\boldsymbol{g}_l^{(i)}\right)^T z_{s,k+1} \leq h_l^{(i)} - \gamma_{k,l}^{(i)} \tag{41}$$

Then the linear constraint (31) can be achieved.

According to ***Assumption 2***, the expectation and variance of $(\boldsymbol{g}_l^{(i)})^T z_{s,k+1}$ can be inferred and its probability distribution function can be determined:

$$\begin{aligned} \boldsymbol{E}\left(\left(\boldsymbol{g}_l^{(i)}\right)^T z_{s,k+1}\right) &= \boldsymbol{E}\left(-s_0^{(i)} - \sum_{j=0}^{k} \dot{x}_j^{(i)} \cdot \tau\right) \\ &= -s_0^{(i)} - (k+1)\mu_l^{(i)}\tau \\ \boldsymbol{D}\left(\left(\boldsymbol{g}_l^{(i)}\right)^T z_{s,k+1}\right) &= \boldsymbol{D}\left(-s_0^{(i)} - \sum_{j=0}^{k} \dot{x}_j^{(i)} \cdot \tau\right) \\ &= (k+1)\tau^2\sigma_l^{2(i)} \\ \left(\boldsymbol{g}_l^{(i)}\right)^T z_{s,k+1} &\sim N(-s_0^{(i)} - (k+1)\,\mu_l^{(i)}\tau, \\ &\quad (k+1)\,\tau^2\sigma_l^{2(i)}) \end{aligned} \tag{42}$$

Therefore, parameter $\gamma_{k,l}^{(i)}$ can be derived through the inverse cumulative distribution function $F_{k,l}^{(i)-1}(\bullet)$, and **Theorem 2** has been proved. ■

Remark 1: If p equals to 0.5, $\gamma_{k,l}^{(i)}$ equals to mean of $\left(\boldsymbol{g}_l^{(i)}\right)^T z_{s,k+1}$, which is usually adopted for deterministic motion control. As a result, this research restricts $p \in [0.5, 1)$.

5) Initial Conditions: In this research, the initial state vector is defined as follows:

$$z(t_0) = \boldsymbol{z_0} \tag{43}$$

$$\boldsymbol{z_0} = [x_0, y_0, \psi_0, v_0, \boldsymbol{\Delta x_0}, \boldsymbol{\Delta y_0}]^{\boldsymbol{T}} \tag{44}$$

E. Solution Method

A solution inspired by dynamic programming is adopted to deal with this problem. This approach was proposed by this research group in a previous study [37]. It can improve computation efficiency greatly by pre-determining the terminal state associated with the optimal solution and using a quadratic fit. In each iteration cycle, this algorithm involves a backward calculation of concomitant matrices and a forward calculation of control vector and state vector. This algorithm is described as follows.

1. Discrete the system dynamics, and calculate $\boldsymbol{A}_k$, $\boldsymbol{B}_k$, for $k \in \{0, 1, \ldots, N\}$

2. Transform (15) in matrix form, $\boldsymbol{Q_k}$ and $\boldsymbol{R}_k$ are weighting matrices of state and control vectors. for $k \in \{0, 1, \ldots, N+1\}$

$$\boldsymbol{Q_k} = \begin{bmatrix} \beta_3 & 0 & 0 & 0 \\ 0 & 0 & 0 & 0 \\ 0 & 0 & \beta_1 & 0 \\ 0 & 0 & 0 & \beta_2 + \beta_4 \end{bmatrix}$$
$$\boldsymbol{R}_k = \begin{bmatrix} \beta_0 & 0 \\ 0 & \beta_0 \end{bmatrix} \tag{45}$$

3. For $k = N + 1$,

$$\begin{aligned} \tilde{\boldsymbol{Q}}_{\boldsymbol{N+1}} &= \boldsymbol{Q}_{\boldsymbol{N+1}} \\ \tilde{\boldsymbol{D}}_{\boldsymbol{N+1}} &= \boldsymbol{0} \\ \tilde{\boldsymbol{E}}_{\boldsymbol{N+1}} &= \boldsymbol{0} \end{aligned} \tag{46}$$

4. For $k \in \{N, N-1, \ldots, 0\}$, calculate the concomitant matrices backward:

$$\begin{aligned} \tilde{\boldsymbol{Q}}_{\boldsymbol{k}} &= \boldsymbol{G}_{\boldsymbol{k}}^{\boldsymbol{T}} \boldsymbol{R}_{\boldsymbol{k}} \boldsymbol{G}_{\boldsymbol{k}} + \boldsymbol{S}_{\boldsymbol{k}}^{\boldsymbol{T}} \tilde{Q}_{\boldsymbol{k+1}} \boldsymbol{S}_{\boldsymbol{k}} + \boldsymbol{Q}_{\boldsymbol{k}} \\ \tilde{\boldsymbol{E}}_{\boldsymbol{k}} &= \frac{1}{2} \boldsymbol{H}_{\boldsymbol{k}}^{\boldsymbol{T}} \boldsymbol{R}_{\boldsymbol{k}} \boldsymbol{H}_{\boldsymbol{k}} + \frac{1}{2} \boldsymbol{T}_{\boldsymbol{k}}^{\boldsymbol{T}} \tilde{Q}_{\boldsymbol{k+1}} \boldsymbol{T}_{\boldsymbol{k}} \\ \tilde{\boldsymbol{D}}_{\boldsymbol{k}} &= \boldsymbol{G}_{\boldsymbol{k}}^{\boldsymbol{T}} \boldsymbol{R}_{\boldsymbol{k}} \boldsymbol{H}_{\boldsymbol{k}} + \boldsymbol{S}_{\boldsymbol{k}}^{\boldsymbol{T}} \tilde{Q}_{\boldsymbol{k+1}} \boldsymbol{T}_{\boldsymbol{k}} + \boldsymbol{S}_{\boldsymbol{k}}^{\boldsymbol{T}} \tilde{D}_{\boldsymbol{k+1}} \\ \boldsymbol{P}_{\boldsymbol{k}} &= \left(\boldsymbol{R}_{\boldsymbol{k}} + \boldsymbol{B}_{\boldsymbol{k}}^{\boldsymbol{T}} \tilde{Q}_{\boldsymbol{k+1}} \boldsymbol{B}_{\boldsymbol{k}} \right)^{-1} \\ \boldsymbol{G}_{\boldsymbol{k}} &= -\boldsymbol{P}_{\boldsymbol{k}} \boldsymbol{B}_{\boldsymbol{k}}^{\boldsymbol{T}} \tilde{Q}_{\boldsymbol{k+1}} \boldsymbol{A}_{\boldsymbol{k}} \\ \boldsymbol{H}_{\boldsymbol{k}} &= -\boldsymbol{P}_{\boldsymbol{k}} \boldsymbol{B}_{\boldsymbol{k}}^{\boldsymbol{T}} \tilde{D}_{\boldsymbol{k+1}} \\ \boldsymbol{S}_{\boldsymbol{k}} &= \boldsymbol{A}_{\boldsymbol{k}} + \boldsymbol{B}_{\boldsymbol{k}} \boldsymbol{G}_{\boldsymbol{k}} \\ \boldsymbol{T}_{\boldsymbol{k}} &= \boldsymbol{B}_{\boldsymbol{k}} \boldsymbol{H}_{\boldsymbol{k}} \end{aligned} \tag{47}$$

5. For $k \in \{0, 1, \ldots, N\}$, calculate control vector and state vector forward:

$$\begin{aligned} \boldsymbol{u}(k) &= \boldsymbol{G}_{\boldsymbol{k}} \boldsymbol{x}(k) + \boldsymbol{H}_{\boldsymbol{k}} \\ \boldsymbol{x}(k+1) &= \boldsymbol{S}_{\boldsymbol{k}} \boldsymbol{x}(k) + \boldsymbol{T}_{\boldsymbol{k}} \end{aligned} \tag{48}$$

Model Predictive Control (MPC) is adopted in order for the implementation of the proposed controller. The proposed controller is applied to find the cost-minimizing control strategy over the entire optimization horizon. Only the control strategy that is within the update horizon shall be implemented, then the state of the surrounding vehicles is sampled again and the calculations are repeated starting from the new current state, yielding a new control and new predicted state path. The proposed controller does not have the full knowledge of the current and future positions of surrounding vehicles. The future positions of surrounding vehicles are predicted using their current states with the consideration of stochasticity. This mechanism not only considers the stochasticity when making predictions on the maneuvering of other vehicles, but also responds rapidly to the deviation of prediction from the reality.

IV. Simulation Evaluation

A. Test Scenario and Settings

In this simulation experiment, all the possible TSP activation scenarios are taken into consideration. A TSP request is made at any second over the cycle length of a signalized intersection, thus an unbiased performance measure can be obtained by averaging the MOE in all possible TSP activation scenarios [38]. The MOE adopted are bus delay and fuel consumption. VT-micro model is utilized to calculate fuel consumption [39].

The formulation of bus delay is formulated as follows:

$$D = \sum_i d_i / C \tag{49}$$

where D is averaged bus delay; d_i is delay if bus arrives at time i.

The formulation of fuel consumption is shown below:

$$\begin{aligned} fuel_i &= \begin{cases} \exp(\sum_{j=0}^{3} \sum_{k=0}^{3} L_{j,k} \cdot v^j \cdot a_x^k) & for\ a_x \geq 0 \\ \exp(\sum_{j=0}^{3} \sum_{k=0}^{3} M_{j,k} \cdot v^j \cdot a_x^k) & for\ a_x < 0 \end{cases} \\ Fuel &= \sum_i fuel_i / C \end{aligned} \tag{50}$$

where Fuel is averaged fuel consumption; $L_{i,j}$ and $M_{i,j}$ are model regression coefficients. $fuel_i$ is fuel consumption if bus arrives at time i.

In addition, one can expect that, the congestion level has an important impact on the experiment results. Therefore, for verifying how the bus delay and fuel consumption change with respect to the different congestion levels, the sensitivity analysis is conducted. Four congestion levels are tested: v/c=0.5, v/c=0.7, v/c=0.9, v/c=1.0.

Settings are as follows:

- The controlled area considers the communication range of DSRC. When the bus reaches 300 meters upstream of the signalized intersection, the controller is activated.
- The signal timing plan is adopted from the practical application in Los Angeles. The cycle length is 90s.
- The speed range of the CAV bus is 0-45 mph.
- the desired speed of background traffic is 45mph.
- p value in the collision avoidance constraint is 0.95.

B. Control Strategies

Four different control strategies are being compared. The purpose of the comparisons is to reveal the advantage of the TSPcut:

- No TSP (NTSP): the regular human-driven bus runs under the background signal timing plan, and no TSP strategy exists.

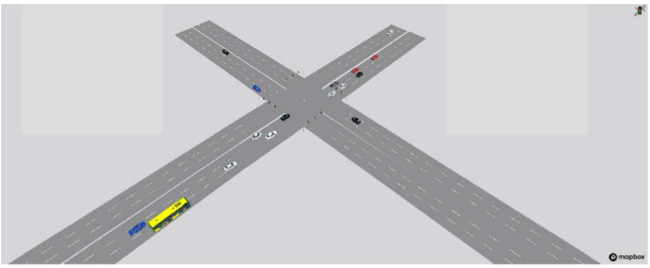

Fig. 5. Microscopic simulation environment in VISSIM.

- Conventional TSP (CTSP): the bus is controlled by human driver, and the conventional TSP logic is adopted. In this simulation experiment, a simple logic (green extension only) without cooperative interactions between the bus and the signal controller is utilized. The CTSP grants 10% of the cycle length as extra green time to all buses which are not early. This TSP logic has been implemented in Los Angeles [1].
- Baseline optimal TSP controller (BocTSP): in this case, the state-of-the-art TSP with CAV bus is adopted. The CAV bus is able to communicate with the signal controller, but only automates longitudinally. No lane-changing nor overtaking maneuver is enabled.
- Proposed controller (TSPcut): both longitudinal and lateral automation are considered. The CAV bus has overtaking capability.

C. Test Bed

It is difficult to conduct numerical analysis to consider the impact of actual traffic condition. A microscopic traffic simulator can assess the performance under more plausible conditions. The off-the-shelf microscopic simulation software VISSIM is used to evaluate the proposed controller under a partially connected and automated environment. In the simulation environment, only the transit bus has the CAV function, and other vehicles are HVs. VISSIM has a whole package of decision-maker and controller that is able to mimic the driving behavior of HVs. For CAV, the bus status, surrounding traffic condition, and TSP timing plan are extracted by external DriverModel and COM interface. The external DriverModel is used to output control commands to the CAV bus. Furthermore, the simulation platform is calibrated for saturation flow rate. It is calibrated to be at 2380 pcu/h/lane.

D. Results

The results of the evaluation are presented in this subsection. The program is coded in MATLAB 2017b and run on an i5-8250U 1.80GHz processor with 8.00GB RAM. The computation time for each optimal control takes about 0.06s. It indicates the proposed controller can potentially be used for real-time applications.

The evaluation results demonstrate that the proposed controller outperforms the NTSP system by up to 49.1% in bus delay savings. This benefit is 3.5% to 16.1% higher than that of the CTSP system and BocTSP system. It means that the TSPcut can take higher advantage of the TSP green time and increase the portion of buses benefiting from TSP logic.

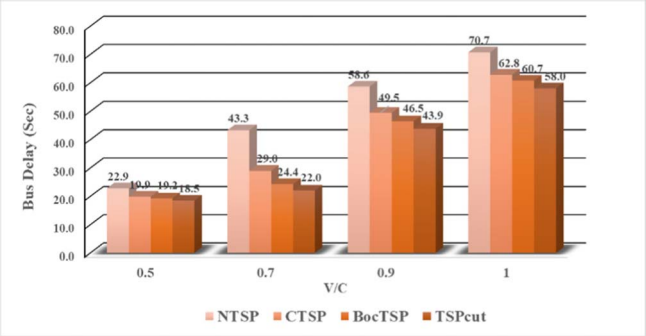

Fig. 6. Bus delay under different congestion levels (Sec).

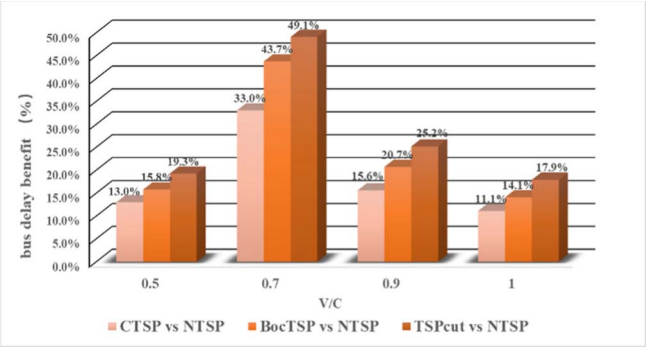

Fig. 7. Bus delay benefits under different congestion levels (%).

In addition, for fuel consumption, the TSPcut can improve by up to 18.4%. These benefits confirm that the TSPcut is able to achieve the aforementioned objectives: reduce bus delay and fuel consumption by optimizing bus trajectory and cooperating with the TSP timing plan.

Fig.6 and Fig.7 respectively show the bus delay and the benefit percentage under different congestion levels. In Fig.6, It is observed that the least bus delay can be achieved when v/c ratio equals to 0.5. With the congestion level rises, bus delay increases correspondingly. The highest bus delay is found when v/c ratio equals 1.0. This phenomenon is due to the fact that the congested traffic provides very limited space for maneuvers, such as overtaking and cut-in. The proposed TSPcut function is practically off during such conditions, as there is not much space for the CAV bus to cut through with. Therefore, congestion level shows a negative impact on the performance of the TSPcut.

In addition, there is an interesting phenomenon found in Fig.7. The greatest delay reduction percentage (49.1%) is observed when v/c ratio equals 0.7. Under the lower congestion level (v/c=0.5), the bus delay is the least, but the benefit percentage is not significant (19.3%). The reason is that under lower congestion level, the bus can naturally catch the TSP green light due to less impact of the traffic flow ahead and queuing. The advantage of the TSPcut is unable to be fully realized under this circumstance. Hence, it is confirmed that the performance of the TSPcut is the most significant when v/c ratio equals 0.7.

The fuel consumption and fuel saving percentage are respectively depicted in Fig.8 and Fig.9. In Fig.8, a phenomenon similar to the one in Fig. 5 can be observed. The fuel consumption increases with the rise of congestion level. In other

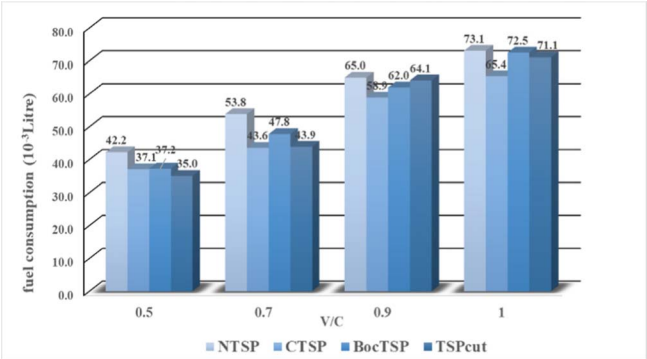

Fig. 8. Fuel consumption under different congestion levels (10^{-3}Litre).

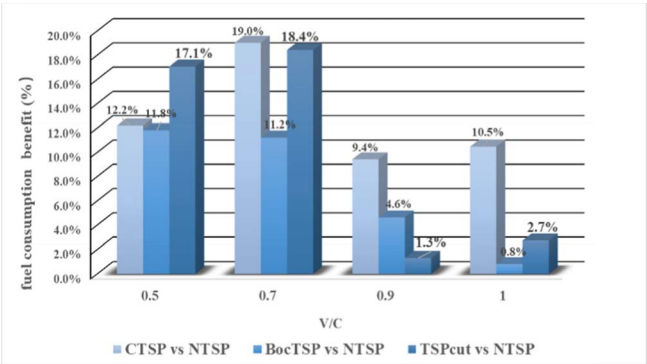

Fig. 9. Fuel consumption benefits under different congestion levels (%).

words, congestion level negatively affects the performance of the proposed TSPcut.

In Fig.9, an interesting phenomenon is observed. The TSPcut can achieve the objective of fuel saving, but the saving percentage is lower than the one brought by CTSP system. When the v/c ratio equals 0.7, 0.9 and 1.0, the fuel saving benefits are 0.6% to 8.1% lower than the CTSP systems. It is because that there is a trade-off between bus delay and fuel consumption. This trade-off can be adjusted by user's preference. As the weighting factor of the fuel saving is set smaller than the one of bus delay in this test case, the controller can sacrifice a small portion of fuel consumption to improve bus delay saving. In addition, under high congestion levels, the off-set of the TSPcut leads to the switch between auto-driving and human-driving. The inappropriate takeover and operation of human driver might result in the increase of fuel consumption.

In the previous test case, it is demonstrated that the greatest performance of TSPcut could be found when v/c=0.7. However, there are also some other important factors that could influence the performance of the proposed controller, including the ego CAV bus's arrival time and the driving speed of the background traffic. Hence, under the optimal congestion level (v/c=0.7), the sensitivity analysis on these two factors is conducted.

1) Sensitivity Analysis on Bus Arrival: Given v/c ratio equals to 0.7 and traffic speed equals to 45mph. Six bus arrival scenarios are tested:

- At the beginning of the green light
- In the middle of the green light
- At the end of the green light

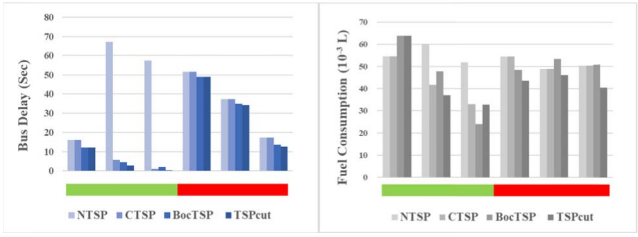

(a) (b)

Fig. 10. Bus delay and fuel consumption under different arrival scenarios.

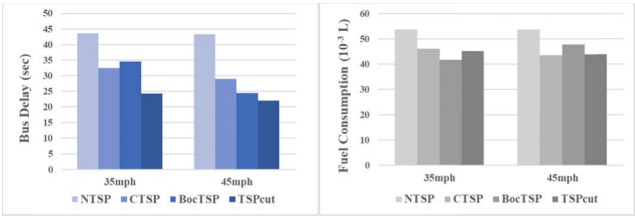

(a) (b)

Fig. 11. Bus delay and fuel consumption under different desired speeds of background traffic.

- At the beginning of the red light
- In the middle of the red light
- At the end of the red light

Fig.10(a) shows the bus delay associated with different arrival time. It is observed that TSPcut is able to significantly reduce bus delay in all arrival scenarios. The most bus delay reduction can be achieved when the ego bus enters the controlled area at the end of the green light. In this arrival scenario, the bus delay under the control of TSPcut is 0.23s. It is a very low value. TSPcut outperforms NTSP by up to 99.6% in bus delay. This benefit mainly results from the TSP green time. Under the same TSP strategy, compared against CTSP and BocTSP, the bus delay reduction is respectively 78.5% and 88.6%. This phenomenon is due to the fact that at the end of the green light, despite the TSP is activated, the rest green time is still not enough. The ego CAV bus has to accelerate immediately to catch the green light. This decision significantly improves mobility and reduces the delay. For BocTSP, the ego bus might be impeded by the HVs in front and cannot achieve its full potential. However, TSPcut also has its limitations. There are times when it sacrifices fuel to reduce delay. This possibility is confirmed in Fig.10(b).

2) Sensitivity Analysis on Traffic Speed: Given v/c ratio equals to 0.7. Two traffic speeds are tested: 35mph and 45mph. The performance is averaged over all possible arrival scenarios.

As shown in Fig.11, TSPcut is able to significantly reduce bus delay under all background traffic speed conditions. The speed of background traffic has a negative impact on bus delay and fuel consumption. As can be expected, the negative impact is more severe on BocTSP than TSPcut. When traffic speed is 35mph, bus delay with BocTSP is 41.4% higher than that in higher-speed traffic flow (45mph). While this impact is only 10.3% for TSPcut. This phenomenon confirms that the CAV bus with BocTSP might lose mobility and miss TSP green light due to the lack of overtaking capability and could be impeded by slow-moving vehicles. This is a proof that the proposed TSPcut is in great need.

V. Conclusion and Future Research

This research proposes a TSPcut controller that enables connected and automated buses to cut through traffic to make TSP green light. The proposed controller overcomes the shortcomings of conventional TSP strategies and is able to: i) overtake slowing moving vehicles in order to catch TSP green time; ii) decide the best time to pass the intersection; iii) considering the stochasticity of surrounding traffic; iv) functional under partially connected and automated environment. It takes full advantage of connected vehicle technology by taking in real-time vehicle and infrastructure information as optimization input. The problem is formulated as an SMPC problem and is solved by a high-efficient dynamic programming algorithm. The nonlinear bicycle model is adopted as the system dynamics to realize CAV bus's lane-changing and overtaking function. The stochasticity of surrounding traffic is considered as a probability distribution which is transformed into a linear chance constraint. Simulation evaluation is conduct to compare the TSPcut against NTSP, CTSP and BocTSP. Sensitivity analysis is conducted for congestion levels. The evaluation results demonstrate that the TSPcut improves the bus delay reduction by 17.9%-49.1%, and the benefits are 3.5% to 16.1% greater than that of other TSP systems. The range is caused by different congestion levels. In addition. Further tests are conducted to analyze how CAV bus's arrival time and the speed of background traffic influence the performance of the TSPcut. Detailed investigation reveals that:

- Congestion level has a negative impact on the performance of the TSPcut.
- The greatest performance of the TSPcut is observed when the v/c ratio equals to 0.7.
- The controller automatically disabled itself when the intersection becomes too congested.
- The most bus delay reduction is observed when the CAV bus arrives at the end of the green light.
- With the decrease of the speed of background traffic, the performance of the TSPcut is more significant.

The proposed controller is applicable to a CAV bus approaching an isolated signalized intersection. Future study could upgrade the controller to enable transit priority over multiple signalized intersections. In addition, the research does not optimize the TSP timing plan. In the future study, the cooperative optimization between bus maneuver and TSP timing plan could be considered.

References

[1] H. R. Smith, B. Hemily, and M. Ivanovic, *Transit Signal Priority (TSP): A Planning and Implementation Handbook*. Washington, DC, USA: ITS America and U.S. Department of Transportation, 2005.

[2] B. Boje and T. Cruikshank, "St. cloud metropolitan transit commission transit priority deployment," in *Proc. 9th World Congr. Intell. Transp. Syst.* Washington, DC, USA: ITS America, 2002, p. 12.

[3] C.-F. Liao and G. A. Davis, "Simulation study of bus signal priority strategy: Taking advantage of global positioning system, automated vehicle location system, and wireless communications," *Transp. Res. Rec., J. Transp. Res. Board*, vol. 2034, no. 1, pp. 82–91, Jan. 2007.

[4] W. Smith and W. Airbrake, "Study of evolutionary urban transportation," US Dept. Housing Urban Develop., Washington, DC, USA, Tech. Rep., 1968, vol. 1.

[5] J. Lee, A. Shalaby, J. Greenough, M. Bowie, and S. Hung, "Advanced transit signal priority control with online microsimulation-based transit prediction model," *Transp. Res. Rec., J. Transp. Res. Board*, vol. 1925, no. 1, pp. 185–194, Jan. 2005.

[6] H. Chatila and M. Swenson, "Transit signal priority along state route 522," in *Proc. ITE Quad Conf.*, Vancouver, BC, Canada, 2001.

[7] R. H. Pratt *et al.*, "Traveler response to transportation system changes: Interim handbook," Transp. Res. Board, Washington, DC, USA, Tech. Rep. TCRP Project B-12, 2000.

[8] K. A. Al-Sahili and W. C. Taylor, "Evaluation of bus priority signal strategies in Ann Arbor, Michigan," *Transp. Res. Rec.*, vol. 1554, pp. 74–79, Jan. 1996.

[9] S. Muthuswamy, W. R. McShane, and J. R. Daniel, "Evaluation of transit signal priority and optimal signal timing plans in transit and traffic operations," *Transp. Res. Rec., J. Transp. Res. Board*, vol. 2034, no. 1, pp. 92–102, Jan. 2007.

[10] M. Garrow and R. Machemehl, "Development and evaluation of transit signal priority strategies," *J. Public Transp.*, vol. 2, no. 2, pp. 65–90, Jun. 1999.

[11] E. C.-P. Chang and C. J. Messer, "Minimum delay optimization of a maximum bandwidth solution to arterial signal timing," Transp. Res. Board, Washington, DC, USA, Technol. Rep. HS-039 135, 1985.

[12] S. Khasnabis, G. V. Reddy, and B. B. Chaudry, "Signal preemption as a priority treatment tool for transit demand management," in *Proc. Vehicle Navigat. Inf. Syst. Conf.*, 1991, pp. 1093–1104.

[13] J. Jacobson and Y. Sheffi, "Analytical model of traffic delays under bus signal preemption: Theory and application," *Transp. Res. B, Methodol.*, vol. 15, no. 2, pp. 127–138, Apr. 1981.

[14] K. N. Balke, C. L. Dudek, and T. Urbanik, "Development and evaluation of intelligent bus priority concept," *Transp. Res. Rec., J. Transp. Res. Board*, vol. 1727, no. 1, pp. 12–19, Jan. 2000.

[15] W. Ekeila, T. Sayed, and M. E. Esawey, "Development of dynamic transit signal priority strategy," *Transp. Res. Rec., J. Transp. Res. Board*, vol. 2111, no. 1, pp. 1–9, Jan. 2009.

[16] G.-L. Chang, M. Vasudevan, and C.-C. Su, "Modelling and evaluation of adaptive bus-preemption control with and without automatic vehicle location systems," *Transp. Res. A, Policy Pract.*, vol. 30, no. 4, pp. 251–268, Jul. 1996.

[17] W. Ma, W. Ni, L. Head, and J. Zhao, "Effective coordinated optimization model for transit priority control under arterial progression," *Transp. Res. Rec., J. Transp. Res. Board*, vol. 2356, no. 1, pp. 71–83, Jan. 2013.

[18] W. Ma, X. Yang, and Y. Liu, "Development and evaluation of a coordinated and conditional bus priority approach," *Transp. Res. Rec., J. Transp. Res. Board*, vol. 2145, no. 1, pp. 49–58, Jan. 2010.

[19] B. Leonard *et al.*, "Connected vehicle deployment-the spat challenge and beyond," in *Proc. ITS Amer. Annu. Meeting Detroit*, 2018.

[20] J. Hu, B. Park, and A. E. Parkany, "Transit signal priority with connected vehicle technology," *Transp. Res. Rec., J. Transp. Res. Board*, vol. 2418, no. 1, pp. 20–29, Jan. 2014.

[21] C. J. Hill and J. K. Garrett, "AASHTO connected vehicle infrastructure deployment analysis," Joint Program Office Intell. Transp. Syst., Washington, DC, USA, Tech. Rep. FHWA-JPO-11-090, 2011.

[22] S. D. Cairano, "An industry perspective on MPC in large volumes applications: Potential benefits and open challenges," *IFAC Proc. Volumes*, vol. 45, no. 17, pp. 52–59, 2012.

[23] M. G. Forbes, R. S. Patwardhan, H. Hamadah, and R. B. Gopaluni, "Model predictive control in industry: Challenges and opportunities," *IFAC-PapersOnLine*, vol. 48, no. 8, pp. 531–538, 2015.

[24] C. E. García, D. M. Prett, and M. Morari, "Model predictive control: Theory and practice—A survey," *Automatica*, vol. 25, no. 3, pp. 335–348, May 1989.

[25] I. A. Ntousakis, I. K. Nikolos, and M. Papageorgiou, "Optimal vehicle trajectory planning in the context of cooperative merging on highways," *Transp. Res. C, Emerg. Technol.*, vol. 71, pp. 464–488, Oct. 2016.

[26] A. Carvalho, Y. Gao, S. Lefevre, and F. Borrelli, "Stochastic predictive control of autonomous vehicles in uncertain environments," in *Proc. 12th Int. Symp. Adv. Vehicle Control*, 2014, pp. 712–719.

[27] A. Gray, Y. Gao, J. K. Hedrick, and F. Borrelli, "Robust predictive control for semi-autonomous vehicles with an uncertain driver model," in *Proc. IEEE Intell. Vehicles Symp. (IV)*, Jun. 2013, pp. 208–213.

[28] X. Lin, D. Gorges, and S. Liu, "Eco-driving assistance system for electric vehicles based on speed profile optimization," in *Proc. IEEE Conf. Control Appl. (CCA)*, Oct. 2014, pp. 629–634.

[29] J. Hu, Y. Shao, Z. Sun, M. Wang, J. Bared, and P. Huang, "Integrated optimal eco-driving on rolling terrain for hybrid electric vehicle with vehicle-infrastructure communication," *Transp. Res. C, Emerg. Technol.*, vol. 68, pp. 228–244, Jul. 2016.

[30] M. Barth, S. Mandava, K. Boriboonsomsin, and H. Xia, "Dynamic ECO-driving for arterial corridors," in *Proc. IEEE Forum Integr. Sustain. Transp. Syst.*, Jun. 2011, pp. 182–188.
[31] X. He, H. X. Liu, and X. Liu, "Optimal vehicle speed trajectory on a signalized arterial with consideration of queue," *Transp. Res. C, Emerg. Technol.*, vol. 61, pp. 106–120, Dec. 2015.
[32] J. B. Rawlings and D. Q. Mayne, *Model Predictive Control: Theory and Design*. Madison, WI, USA: Nob Hill Publishing, 2009.
[33] M. Morari, C. E. Garcia, and D. M. Prett, "Model predictive control: Theory and practice," *IFAC Proc. Volumes*, vol. 21, no. 4, pp. 1–12, Jun. 1988.
[34] J. Kong, M. Pfeiffer, G. Schildbach, and F. Borrelli, "Kinematic and dynamic vehicle models for autonomous driving control design," in *Proc. IEEE Intell. Vehicles Symp. (IV)*, Jun. 2015, pp. 1094–1099.
[35] H. X. Liu, X. Wu, W. Ma, and H. Hu, "Real-time queue length estimation for congested signalized intersections," *Transp. Res. C, Emerg. Technol.*, vol. 17, no. 4, pp. 412–427, Aug. 2009.
[36] J. Hu, B. B. Park, and Y.-J. Lee, "Coordinated transit signal priority supporting transit progression under connected vehicle technology," *Transp. Res. C, Emerg. Technol.*, vol. 55, pp. 393–408, Jun. 2015.
[37] H. Wang, X. Li, Y. Zhang, B. Sun, W. Ma, and J. Hu, "Motion planning algorithm under partially connected and automated environment," in *Proc. Transp. Res. Board 98th Annu. Meeting*, 2019, p. 5.
[38] J. Hu, B. B. Park, and Y.-J. Lee, "Transit signal priority accommodating conflicting requests under connected vehicles technology," *Transp. Res. C, Emerg. Technol.*, vol. 69, pp. 173–192, Aug. 2016.
[39] H. Rakha, K. Ahn, and A. Trani, "Development of VT-micro model for estimating hot stabilized light duty vehicle and truck emissions," *Transp. Res. D, Transp. Environ.*, vol. 9, no. 1, pp. 49–74, Jan. 2004.

Jia Hu (Member, IEEE) is currently working as the Zhongte Distinguished Chair of Cooperative Automation with the College of Transportation Engineering, Tongji University. Before joining Tongji University, he was a Research Associate with the Federal Highway Administration (FHWA), USA. Furthermore, he is also a member of TRB (a division of the National Academies) Vehicle Highway Automation Committee, Freeway Operation Committee, and Simulation subcommittee of Traffic Signal Systems Committee, and a member of CAV Impact Committee and Artificial Intelligence Committee of the ASCE Transportation and Development Institute. He is also an Associate Editor of the American Society of Civil Engineers *Journal of Transportation Engineering* and IEEE OPEN JOURNAL IN INTELLIGENT TRANSPORTATION SYSTEMS, an Assistant Editor of the *Journal of Intelligent Transportation Systems*, and an Advisory Editorial Board Member of the *Transportation Research Part C: Emerging Technologies*. He has been an Associate Editor of the IEEE Intelligent Vehicles Symposium since 2018 and the IEEE Intelligent Transportation Systems Conference since 2019.

Zihan Zhang was born in Shanghai, China. He received the B.S. degree in traffic engineering from Dalian Maritime University, Dalian, China, in 2018. He is currently pursuing the Ph.D. degree with Tongji University. His research interests include connected and automated vehicle, ITS, optimal control theory, eco-driving, and human-like decision-making and control.

Yongwei Feng was born in Henan, China. He received the B.S. degree in traffic engineering from Tongji University in 2020, where he is currently pursuing the master's degree. His research interests include connected and automated vehicle, optimal control theory, and ITS.

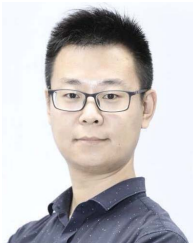

Zhongxiao Sun worked as an Automotive Industry Solution Expert with Suzhou Tongyuan Soft Control Information Technology Company Ltd. Before that, he also had rich leadership experiences in leading his team focus on ADAS decision and function software development. He has acquired over 18 patents during this period. He is currently an expert in the field of industry and information technology and industrial internet in Suzhou. Furthermore, he wrote a book on Simulink Simulation and Code Generation which was published in 2015.

Xin Li received the Ph.D. degree from UW-Milwaukee in 2015. He is currently employed as the "Xinghai" Professor with the College of Transportation Engineering, Dalian Maritime University, and the Collaborative Innovation Center for Transport Study, Dalian Maritime University. He is also a Transportation Researcher with expertise in traffic network design and system performance evaluation. Prior to serving in Dalian Maritime University, he was a Post-Doctoral Researcher with The Hong Kong Polytechnic University. He also gained professional experience at a major consulting firm in U.K. He also has agency experience from his years at the in-house consulting service for the metropolitan government of Chongqing, China.

Xianfeng (Terry) Yang (Member, IEEE) received the B.S. degree in civil engineering from Tsinghua University in 2009 and the M.S. and Ph.D. degrees in civil engineering from the University of Maryland, College Park, MD, USA, in 2011 and 2015, respectively. He is currently an Assistant Professor with the Department of Civil & Environmental Engineering, The University of Utah. His research interests include machine learning applications in transportation engineering, traffic operations under connected automated vehicle environment, traffic flow modeling, integrated traffic control, traffic signal optimization, and emergency evacuation modeling. His research is sponsored by the U.S. Department of Transportation (USDOT), the Federal Highway Administration (FHWA), the National Science Foundation (NSF), and the Utah Department of Transportation (UDOT). He is also a member and a paper review coordinator of two TRB standing committees, AHB25 Traffic signal systems, and ABR30 Emergency Evacuations, and the Vice Chair of the INFORMS TSL/SIG-Intelligent Transportation System Committee. He received the NSF CAREER Award in 2021. He is also the Associate Editor of ASCE *Journal of Urban Planning and Development* and IEEE OPEN JOURNAL OF INTELLIGENT TRANSPORTATION SYSTEMS, the Handling Editor of JOURNAL OF TRANSPORTATION RESEARCH BOARD: TRANSPORTATION RESEARCH RECORD, and the Editorial Board Member of *Transportation Research Part C: Emerging Technologies*.